American Journal of Pathology, Vol. 147, No. 3, September 1995
Copyright © American Society for Investigative Pathology

Active Proliferation of Different Cell Types, Including Lymphocytes, in Human Atherosclerotic Plaques

Mark D. Rekhter and David Gordon

From the Department of Pathology, University of Michigan, Ann Arbor, Michigan

Cell proliferation, an important mechanism of atherosclerotic plaque growth, occurs among smooth muscle, inflammatory cell, and other cell types. We have identified different topographical patterns of cell proliferation in human carotid plaques, based on cell type. Cell proliferation was determined with an antibody to the proliferating cell nuclear antigen (PCNA), combined with cell type-specific antibodies. Despite low levels of overall proliferative activity, the intima displayed more proliferative activity than the underlying media (1.61 ± 0.35% in intima versus 0.05 ± 0.03% in media; P < 0.01). The preponderant proliferative cell type in the intima was the monocyte/macrophage (46.0% of PCNA-positive cells), with a minority being smooth muscle α-actin-positive (9.7%), microvascular endothelial (14.3%), and T cells (13.1%). Smooth muscle cells were the dominant proliferating cell type in the media (44.4% of PCNA-positive cells versus 20% endothelial cells, 13.0% monocyte/macrophages, and 14.3% T cells). Within the plaque, foam-cell-rich regions mostly displayed proliferation among macrophages (66.5%), whereas in vascularized fields PCNA positivity was almost equally shared by endothelial cells (23.8%), monocyte/macrophages (26.3%), smooth muscle α-actin-positive cells (14.0%), and to a lesser extent, T cells (8.2%). Logistic and linear regression analyses also demonstrated that location in foam-cell-rich regions was a significant predictor of proliferation only among monocyte/macrophages, whereas location in vascularized regions was a good predictor of PCNA positivity among both inflammatory and noninflammatory cells. These different patterns of cell type proliferation suggest possibly different distributions of putative responsible growth regulatory factors in human atherosclerosis. (Am J Pathol 1995, 147:668–677)

Previous studies from this laboratory and others have indicated the focal low levels of cell proliferation in human atherosclerotic plaques.[1,2] We have also observed that cell proliferation occurs among smooth muscle, inflammatory cell, and other cell types.[1] The above analyses were applied to the whole plaque irrelevant to particular plaque regions. However, atherosclerotic plaques are very complex structures, which consist of several morphologically distinct areas (fibrous cap, necrotic core, vascularized regions, etc).[3] Yet none have tried to map actual cell proliferation within the plaque. In the present paper, we have identified different topographical patterns of cell proliferation in human carotid plaques, on the basis of cell type.

Materials and Methods

Tissue Preparation

We studied samples of advanced, complicated, human carotid artery plaques removed at the time of endarterectomy surgery. Although all lesions exhibited significantly stenosing plaques, none showed total occlusion. As control arterial tissue, portions of human internal mammary artery left over from coronary bypass surgery were obtained. The final study set consisted of 11 carotid plaques and 10 internal mammary arteries. These studies were approved by the Human Subjects Review Committees, both at the University of Michigan (Ann Arbor, MI) and at the

Supported by National Institutes of Health grant HL 42119 and a grant-in-aid from the American Heart Association.

Accepted for publication May 15, 1995.

Address reprint requests to Dr. David Gordon, Department of Pathology, The University of Michigan, M3225 Med.Sci. I, 1301 Catherine, Ann Arbor, MI 48109-0602.

University of Washington (Seattle, WA), the institutional sources of these tissue samples. Specimens were fixed overnight in methanol-Carnoy's fixative (methanol:chloroform:glacial acetic acid in a 60:30:10 volume ratio), decalcified in 2% L-ascorbic acid for 3 days, paraffin embedded and sectioned at 5 μm thickness. Depending on the size of the sample, one to three cross-sectional slices of artery were thus placed in each tissue block (ie, one block per patient) from which several serial sections were generated for hematoxylin and eosin staining as well as the subsequent immunocytochemistry studies. Obviously, the carotid plaque portions that we received were deemed by the surgeon to be the most obstructive parts in the patients carotid bifurcation region. Our study sections were from this central, stenotic portion of these resected plaques. Within this plaque region, we designated each of our microscopic fields as being within certain regions such as the media *versus* intima and, within the intima, as being in the fibrous cap zone, in foam-cell-rich regions, or in vascularized zones.

Immunocytochemistry

Reagents

As a marker of cell proliferation, anti-proliferating cell nuclear antigen (PCNA) antibody was used (PC10, Dako Corp., Carpinteria, CA). The cell-type-specific antibodies used on these tissues were anti-smooth muscle α-actin antibody (Boehringer Mannheim Corp., Indianapolis, IN) to identify smooth muscle cells, CD68 (DAKO-CD68, KP1, Dako) to identify macrophages, CD3 (Dako) for T lymphocytes, and biotinylated Ulex Europaeus agglutinin I (Vector Laboratories, Burlingame, CA) to identify endothelial cells. Biotinylated horse anti-mouse and goat anti-rabbit antibodies, avidin-biotin-peroxidase complex (ABC), alkaline phosphatase-conjugated streptavidin, normal (nonimmune) horse and goat sera, and the alkaline phosphatase substrate kit (red) were obtained from Vector Laboratories. Normal mouse and rabbit sera were provided by Immunon (Pittsburgh, PA). 3′,3′-Diaminobenzidine was obtained from Sigma Chemical Co.(St. Louis, MO) and clearing agent Histoclear was from National Diagnostics (Atlanta, GA).

Immunostaining

Single-label immunocytochemistry was performed as previously described.[4,5] Sections were deparaffinized and endogenous peroxidase activity was blocked with H_2O_2 for 5 minutes. With 2% normal horse serum as diluent, mouse anti-human PC10 antibody (dilution 1:1000) was applied overnight at 4°C. The secondary antibody incubation (biotinylated horse anti-mouse antibody, dilution 1:1000) was for 3 hours at 4°C followed by avidin-biotin amplification (ABC kit) for 30 minutes. Incubation with 0.1% 3′,3′-diaminobenzidine and H_2O_2 at room temperature for 5 to 10 minutes produced a brown reaction product. Light hematoxylin counterstain was used to visualize all nuclei in the tissue sections.

For double-labeled immunocytochemistry, the above described protocol was followed when separate cell structures were to be labeled. The first immunostaining procedure (PCNA) was carried out as described above, except that 8% nickel chloride was added into the solution of diaminobenzidine to obtain a black reaction product (to increase contrast). After the first immunostaining procedure, the sections were washed copiously in phosphate-buffered saline and the second primary antibody (mouse anti-pig α-actin antibody at 1:1000 dilution in 2% normal horse serum, mouse anti-human CD68 antibody at 1:1000 dilution in 2% normal horse serum, or rabbit anti-human CD3 antibody at 1:100 dilution in 2% normal goat serum) was applied overnight at 4°C. The biotinylated secondary antibody to the second primary antibody (biotinylated horse anti-mouse antibody, dilution 1:500, or biotinylated goat anti-rabbit antibody at 1:500 dilution in 2% normal horse serum) was then applied for 3 hours at 4°C, followed by another 30-minute incubation in streptavidin-alkaline phosphatase (diluted at 1:1000) and then developed with the alkaline phosphatase substrate, which produced a red reaction product. For endothelial cell staining, the sections were incubated overnight at 4°C with biotinylated Ulex Europaeus agglutinin I at 1:100 dilution and then transferred directly to streptavidin-alkaline phosphatase, incubated, and developed as described above. Methyl green counterstain was used to visualize nuclei in the tissue sections.

PCNA Control

We have previously performed numerous PCNA immunostainings on different tissues with excellent reproducibility. Our protocol has provided stable cell numbers over a range of antibody dilutions, and the 1:1000 dilution provides the best signal-to-background staining ratio. As previously described with a different PCNA antibody[1] in-house studies with the current antibody have revealed a good correlation with thymidine labeling of rat intestine, and the rat

intestine control tissue is run with each PCNA immunostaining run and always reveals specific nuclear staining localized to the crypt epithelium of the intestinal mucosa (data not shown). Human tonsil was also used as a control tissue and gave positive staining primarily in the follicular centers as expected. Using a different proliferation-specific antibody to Ki-67 antigen,[6] we have also obtained very similar levels and patterns of staining on both human carotid plaques and tonsil tissue (data not shown). Additional control immunoreactions on this tissue included the use of normal mouse serum, which gave no staining.

Cell-Type-Specific Antibodies Control

As a positive tissue control for α-actin, rat intestine was used with every run and gave the expected well localized pattern within tunica muscularis with negative staining of epithelial elements and fibroblasts (data not shown). Human tonsil and spleen were similarly used as controls for all cell-type-specific antibodies. α-Actin staining was mostly concentrated around the blood vessels, CD68-positive cells demonstrated typical macrophage localization and morphology, CD3-positive cells demonstrated lymphocyte-like appearance and T-cell-specific periarteriolar localization on the spleen sections, and Ulex Europaeus agglutinin I specifically revealed microvascular endothelial cells (data not shown). Additional control immunoreactions on these tissues included the use of normal mouse and rabbit serum, which gave no staining.

Control of Double-Label Procedure

Double labeling was performed at the same time as single labeling with each individual antibody (ie, PCNA, α-actin, CD68, CD3, and Ulex agglutinin) on the serial sections. Patterns of individual antibody immunoreactions on double-labeled slides corroborated the patterns of their single-labeled counterparts. Additionally, the various antibodies used (all IgGs) served as nonspecific IgG staining controls for each other and each provided distinctly different patterns (eg, smooth muscle *versus* macrophage distributions) and, except for the PCNA antibody, did not give nuclear localizations.

Morphometric Analysis

To quantitatively study the distribution of PCNA-positive cells, the single- and double-labeled tissue sections were studied by light microscopy at ×400 magnification with the Image 1 system of computer color image analysis (Universal Imaging Corp., West Chester, PA). Contiguous, nonoverlapping microscopic fields were analyzed covering the whole tissue on the slide. On the single-labeled slides, each field was scored for (1) total number of nuclei, (2) number of PCNA-positive nuclei, and (3) location in intima or media.

The average PCNA index per sample was then used to calculate the statistical comparisons of the intimas and medias within the plaques. These data were compared by Student's *t*-test.

On the double-labeled slides, each field was scored for (1) number of PCNA-positive nuclei, (2) number of PCNA-positive nuclei associated with cytoplasm positive for certain cell-type-specific markers (ie, proliferating smooth muscle cells, monocyte/macrophages, T lymphocytes, and endothelial cells), (3) location in intima or media, (4) location in the fibrous cap, (5) location in a foam-cell-rich area, and (6) presence of microvessels. Variables 3 to 6 were scored on a present (1) or absent (0) basis.

To answer the question of what plaque features are the best predictors of different cell type proliferation, we used both logistic regression and multiple linear regression analyses, with the microscopic field-by-field data sets. For each combination of immunostains (PCNA plus α-actin, PCNA plus Ulex, etc), we combined all of the microscopic field data from all 11 carotid plaques into one large data set. We recognized that the above pooling of field-by-field data sets assumes that each microscopic field is an independent event, even if separate fields came from the same plaque. Because we were concerned that this assumption might not be valid, separate identification variables for each plaque were also included. These were assigned as follows: ID1 = 1 for carotid plaque from patient 1, ID2 = 2 for carotid plaque from patient 2, etc, with the plaque from patient 11 being indicated by ID1-ID10 all having a value of zero. To determine predictors of the presence *versus* absence of PCNA within a microscopic field, immunostainable PCNA in cells of a certain type in a given microscopic field was coded as a yes/no variable and used as the outcome variable.

To determine predictors of the number of proliferating cells of different types, multiple linear regression was performed with the number of PCNA-positive cells per microscopic field used as the outcome variable. For every combination of immunostains, all microscopic field data from all 11 carotid plaques were pooled into one data sample. The

independent variables (defined above) were the microscopic field presence/absence of foam cells, location in the fibrous cap, plaque microvessels, and presence in the media. Because of multiple colinearity problems we were not able to include the specimen identification variables in this particular analysis.

Statistical analysis was performed with the statistical package True Epistat (Epistat Services, Richardson, TX).

Results

Overall Cell Proliferation

Internal mammary arteries used as examples of nonpathological human artery were without significant intimal thickening. In agreement with previous reports,[7,8] no PCNA-positive cells were found. The human carotid plaque samples exhibited features of advanced, complicated atherosclerotic plaques, including focal neovascularization, necrotic cores, and calcification. Occasional focal regions of thrombus and/or hemorrhage, of varying ages, were also seen. Only a very thin rim of media (three to four elastic laminae in width) was attached. In these plaques, very few PCNA-positive cells were seen. Positive cells were often randomly located as single cells with occasional clusters. Intima had a greater proportion of PCNA-positive cells than did media (mean ± SE, 1.61 ± 0.35% in intima *versus* 0.05 ± 0.03% in media; Figure 1). This difference was statistically significant ($P < 0.01$, by either independent or paired *t*-tests). According to the visual impression, PCNA-positive cells were more often seen in the foam-cell-rich regions around the necrotic core and in vascularized regions, although this pattern was not always obvious.

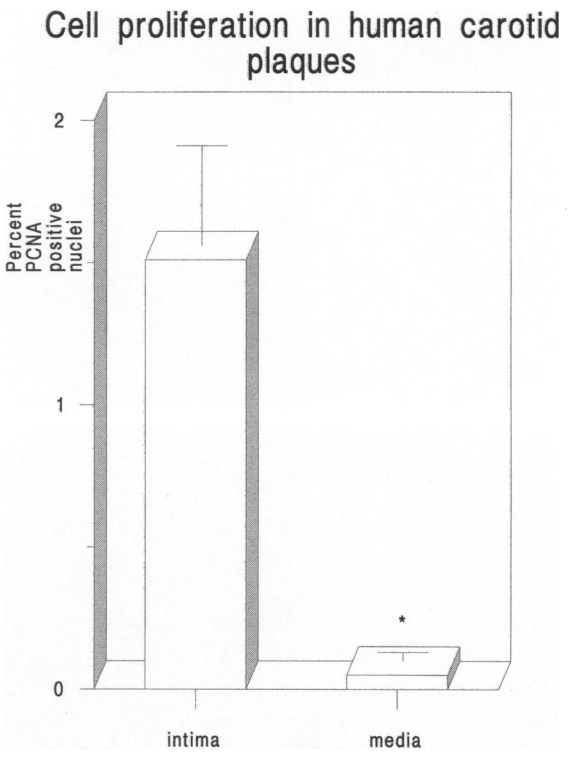

Figure 1. *Comparison of the mean percentage of PCNA-positive cells.* *P < 0.01

Cell Types Displaying PCNA Reactivity

We also performed double-label immunocytochemistry with anti-PCNA and cell-type-specific antibodies on human carotid plaques to identify the cell types displaying PCNA immunostaining (Figure 2 and Table 1). The preponderant proliferative cell type in the intima was the monocyte/macrophage (46.0% of PCNA-positive cells), with a minority being smooth muscle α-actin positive (9.7%), microvascular endothelial (14.3%), and T cells (13.1%). Smooth muscle cells were the dominant proliferating cell type in the media (44.4% of PCNA-positive cells *versus* 20% endothelial cells, 13.0% monocyte/macrophages, and 14.3% T cells). Within the plaque, foam-cell-rich regions mostly displayed proliferation among macrophages (66.5%), whereas in vascularized fields PCNA positivity was almost equally shared by endothelial cells (23.8%), monocyte/macrophages (26.3%), smooth muscle α-actin-positive cells (14.0%), and to a lesser extent, T cells (8.2%). The fibrous cap region of the plaque (where the overall rate of cell proliferation was minimal) displayed proliferation among T cells (34.1%), monocyte/macrophages (14.5%), and smooth muscle α-actin-positive cells (11.0%). We did not observe proliferation among luminal endothelial cells, but this might reflect a massive luminal endothelial loss induced by the endarterectomy procedure, rather than real quiescence of this part of the plaque tissue.

Quantitative Analyses of Colocalization within the Same Microscopic Fields

For an analysis of different cell type proliferation by plaque topographical features, all of the microscopic field data from all carotid plaques were pooled and analyzed first by logistic regression with the presence/absence of immunostainable PCNA (associated with a certain cell-type marker) in each microscopic field being the outcome variable (Table 2). If a cut-off predicted probability (of presence) of 0.5

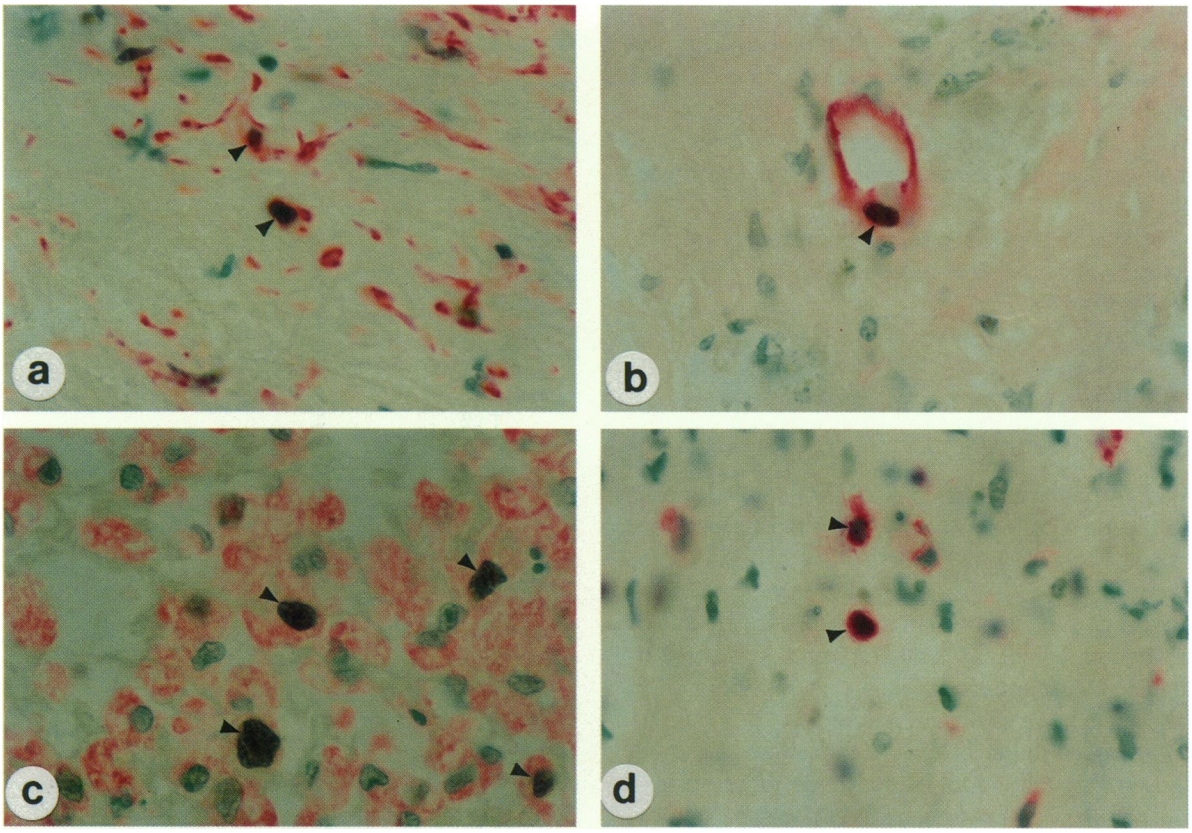

Figure 2. *Cell types displaying PCNA reactivity in human carotid atherosclerotic plaques (according to double-label immunocytochemistry). Magnification ×680 (100× objective).* **a:** *Double immunolabeling for PCNA and α-actin. Several cells exhibit black PCNA-positive nuclei (product of peroxidase reaction, shown with arrowhead) and red α-actin-positive cytoplasm (product of alkaline phosphatase reaction). Light green counterstain shows PCNA-negative nuclei.* **b:** *Double immunolabeling for PCNA and endothelial cell-specific marker Ulex Europaeus agglutinin 1. Note black PCNA-positive nucleus (arrowhead) surrounded by red Ulex-positive cytoplasm.* **c** *and* **d:** *Proliferation of the inflammatory cells in the atherosclerotic plaque. Note black PCNA-positive nuclei (arrowheads) surrounded by red cell-type-specific protein cytoplasm. Double immunolabeling for PCNA and CD68 (monocyte/macrophage) antigen is shown in* **c** *and CD3 (T cells) antigen is shown in* **d**.

was used, the overall logistic regression model provided a good fit to the data, correctly classifying 94.0% of microscopic fields (when the presence of proliferating α-actin-positive cells was an outcome variable), 90.6% of microscopic fields (when the presence of proliferating endothelial cells was an outcome variable), 84.2% of microscopic fields (when the presence of proliferating monocyte/macrophages was an outcome variable), and 94.5% of microscopic fields (when the presence of proliferating T cells was an outcome variable). Of all of the independent microscopic field variables noted (presence of microvessels, foam cells, fibrous cap location, location within the intima, and sample-specific identifiers), location in foam-cell-rich regions was a significant predictor of proliferation only among monocyte/macrophages (Table 2C), whereas location in vascularized regions was a good predictor of PCNA positivity among both inflammatory and noninflammatory cells, as indicated by *P*

Table 1. *Cell Type Composition of PCNA-Positive Cells in Human Carotid Plaques*

	Percentage of each cell type category in PCNA-positive cells (%),				
	α-Actin (smooth muscles)	Ulex Europaeus I (endothelial cells)	CD68 (macrophages)	CD3 (T cells)	Undefined cells*
Intima	9.7	14.3	46.0	13.1	16.9
Media	44.4	20.0	13.0	14.3	8.3
Foam	2.6	3.2	66.5	7.5	20.0
Cap	11.0	0	14.5	34.1	40.0
Vascularity	14.0	23.8	26.3	8.2	27.7

*Percentage of undefined cells is estimated by subtracting the actual percentage of proliferating α-actin-positive cells, endothelial cells, monocyte/macrophages, and T cells from 100%.

Table 2. *Logistic Regression Analysis on All Human Carotid Plaque Microscopic Fields.*

Independent variable	Coefficient	Odds ratio	*P* value	Independent variable	Coefficient	Odds ratio	*P* value
A*				C‡			
Foam cells	−0.5067	0.6025	0.2944	**Foam cells**	**3.2044**	**24.6399**	**<0.0001**
Cap	0.3440	1.4106	0.5054	Cap	0.4981	1.6457	0.3561
Vascularity	**2.1260**	**8.3815**	**<0.0001**	**Vascularity**	**1.9711**	**7.1783**	**<0.0001**
Media	0.1666	1.1813	0.7909	Media	−0.2427	0.7845	0.7234
ID1	0.7698	2.1593	0.3515	ID1	−13.0072	0.000002	0.9716
ID2	0.0524	1.0538	0.9535	ID2	0.5156	1.6746	0.5385
ID3	−0.0917	0.9124	0.9097	**ID3**	**1.5419**	**4.6737**	**<0.05**
ID4	0.0227	1.0230	0.9800	ID4	1.0329	2.8091	0.2246
ID5	**1.6958**	**5.4510**	**<0.01**	**ID5**	**1.7285**	**5.6323**	**<0.05**
ID6	−1.2115	0.2977	0.2907	ID6	1.5976	4.9412	0.0658
ID7	−0.9281	0.3953	0.4165	**ID7**	**2.0899**	**8.0837**	**<0.01**
ID8	**1.5122**	**4.5369**	**<0.05**	**ID8**	**2.7010**	**14.8942**	**<0.001**
ID9	−0.4271	0.6524	0.7132	ID9	1.7952	6.0209	0.0161
ID10	−0.1759	0.8387	0.8449	ID10	−0.8885	0.04113	0.4844
B†				D§			
Foam cells	0.6623	1.9392	0.1871	Foam cells	0.9176	2.5033	0.1407
Cap	−12.9121	0.0000025	0.9779	**Cap**	**1.6516**	**5.2153**	**<0.05**
Vascularity	**4.5062**	**90.5741**	**<0.0001**	**Vascularity**	**2.9652**	**19.3988**	**<0.0001**
Media	−0.1272	0.8805	0.8515	Media	−1.2183	0.2957	0.3002
ID1	−3.3295	0.0358	0.0034	ID1	−0.5918	0.5533	0.9996
ID2	−2.8589	0.0573	0.0155	ID2	−0.2798	0.7560	0.9998
ID3	−0.9414	0.3901	0.1010	ID3	13.5441	762270.53	0.9880
ID4	−1.0419	0.3528	0.1824	ID4	14.7844	2634893.1	0.9869
ID5	1.1877	3.2794	0.1951	ID5	16.2104	1097000.0	0.9857
ID6	−0.6018	0.5478	0.4640	ID6	13.2566	571829.01	0.9883
ID7	**−2.5524**	**0.0779**	**<0.001**	ID7	−0.3125	0.7316	0.9998
ID8	0.1687	1.1837	0.8136	ID8	15.1227	3695628.3	0.9866
ID9	−0.9480	0.3875	0.1684	ID9	14.5281	2039342.4	0.9872
ID10	−1.2785	0.2785	0.1315	ID10	−0.0061	0.9939	1.0000

*All microscopic field data from all 11 carotid plaques were pooled into one data sample. Thus, a total of 637 fields were analyzed. The independent variables (defined in Materials and Methods) correlated with the outcome variable are listed above, with the calculated regression coefficients, associated odds ratios, and statistical *P* values of each to the overall regression analysis. In addition, specimen identity variables were also included as described in Materials and Methods, with ID1 referring to fields from carotid sample 1, ID2 referring to fields from carotid sample 2, etc. The overall regression statistics are as follows: χ^2 = 74.0197, df = 14, and $P < 0.0001$. The comparison of this model with the actual data obtained (using all variables with the above coefficients to predict the outcome variable) shows that the model accounts for 21.30% of the log likelihood, a goodness of fit χ^2 = 50.6861, df = 3, $P < 0.0001$, and a correct classification of the outcome variable of 94.0% given a cut-off probability of 0.5. In A, the outcome variable was the presence or absence of at least one PCNA-positive α-actin-positive cell (coded on a yes/no basis).

†A total of 763 fields were analyzed. The overall regression statistics are as follows: χ^2 = 202.8779, df = 14, and $P < 0.0001$. The comparison of this model with the actual data obtained (using all variables with the above coefficients to predict the outcome variable) shows that the model accounts for 47.35% of the log likelihood, a goodness of fit χ^2 = 35.1854, df = 7, $P < 0.001$, and a correct classification of the outcome variable of 90.6% given a cut-off probability of 0.5. In B, the outcome variable was the presence or absence of at least one PCNA-positive endothelial (Ulex Europaeus agglutinin I-positive) cell (coded on a yes/no basis).

‡A total of 665 fields were analyzed. The overall regression statistics are as follows: χ^2 = 226.0129, df = 14, and $P < 0.0001$. The comparison of this model with the actual data obtained (using all variables with the above coefficients to predict the outcome variable) shows that the model accounts for 36.53% of the log likelihood, a goodness of fit χ^2 = 71.5249, df = 6, $P < 0.0001$, and a correct classification of the outcome variable of 84.2% given a cut-off probability of 0.5. In C, the outcome variable was the presence or absence of at least one PCNA-positive monocyte/macrophage (CD68-positive cell), coded on a yes/no basis.

§A total of 549 fields were analyzed. The overall regression statistics are as follows: χ^2 = 81.9368, df = 14, and $P < 0.0001$. The comparison of this model with the actual data obtained (using all variables with the above coefficients to predict the outcome variable) shows that the model accounts for 37.04% of the log likelihood, a goodness of fit χ^2 = 36.8226, df = 6, $P < 0.0001$, and a correct classification of the outcome variable of 94.5% given a cut-off probability of 0.5. In D, the outcome variable was the presence or absence of at least one PCNA-positive T cell (CD3-positive cell), coded on a yes/no basis.

values of <0.05 and odds ratios of >1. (Table 2, A–D). For proliferating T cells, location in fibrous cap region also was a significant predictor (Table 2D). Sometimes plaque identity had an apparent effect on these correlations. Two plaques (ID5 and ID8) appeared to have significant and independent association with α-actin-positive cell proliferation (Table 2A). Only one plaque (ID7) showed significant, albeit negative, association with endothelial cell proliferation (Table 2B). Four plaques (ID3, -5, -7, and -8) exhibited independent association with proliferation of monocyte/macrophages (Table 2C). Neither plaque identifier served as independent predictor of T cell proliferation (Table 2D).

The above logistic regression analysis indicates likelihoods of finding at least one PCNA-positive cell of certain type per microscopic field but says nothing about the number of positive cells found. To assess this, multiple linear regression was performed on these same pooled carotid plaque fields, with the

Table 3. *Overall Multiple Linear Regression for All Carotid Plaque Microscopic Fields*

Outcome variable	Independent variable	Coefficient	SEM	*P* value
Number of proliferating α-actin-positive cells	Foam cells	−0.0355	0.0216	0.1002
	Cap	0.0056	0.0232	0.8088
	Vascularity	0.1783	0.0245	<0.001
	Media	−0.0045	0.0260	0.8611
Number of proliferating endothelial cells	Foam cells	−0.1577	0.0785	<0.05
	Cap	−0.0524	0.0859	0.5422
	Vascularity	0.7268	0.0714	<0.001
	Media	−0.0153	0.0865	0.08594
Number of proliferating monocyte/macrophages	Foam cells	1.0114	0.1049	<0.001
	Cap	0.0632	0.1358	0.6418
	Vascularity	0.4156	0.1319	<0.01
	Media	0.0182	0.1253	0.8847
Number of proliferating T cells	Foam cells	0.1336	0.0899	0.1377
	Cap	0.2875	0.0922	<0.01
	Vascularity	0.1729	0.1022	0.0912
	Media	−0.0167	0.0896	0.8525

All microscopic data from all 11 carotid plaques were pooled into one data sample. The outcome variable was the number of proliferating cells of different types (α-actin-positive cells, endothelial cells, monocyte/macrophages, and T cells) per microscopic field. A total 637 fields were analyzed for PCNA-positive α-actin-positive cells, 763 fields for PCNA-positive endothelial cells, 665 fields for PCNA-positive monocyte/macrophages, and 549 fields for PCNA-positive T cells. The independent variables (defined in Materials and Methods) were the microscopic field presence/absence of the following: foam cells, location in the fibrous cap, plaque microvessels, and appearance in the media. These are listed with their calculated coefficients, SEM, and *P* value of significance to the overall regression. Because of multiple colinearity problems, we were not able to include the specimen identification variables in this particular analysis.

number of PCNA-positive cells of different types per field as the quantitative outcome variable (summarized in Table 3). Again, vascularity is still highlighted as a significant variable for both inflammatory and noninflammatory cells. In agreement with logistic regression data, location in foam-cell-rich regions was a significant predictor of proliferation only among monocyte/macrophages. However, these regression models account for only 7.31% of the PCNA variation seen for proliferating α-actin-positive cells, 17.08% for proliferating endothelial cells, 15.40% for proliferating monocyte/macrophages, and 2.47% for proliferating T cells, respectively.

Thus, both logistic and linear regression analyses demonstrated that location in foam-cell-rich regions was a significant predictor of proliferation only among monocyte/macrophages, whereas location in vascularized regions was a good predictor of PCNA positivity among both inflammatory and noninflammatory cells.

Discussion

In this report, we used the antibody to the cell-cycle-related protein, PCNA, to determine the level of cell proliferation in human carotid atherosclerotic plaques. PCNA is an auxiliary protein of mammalian DNA polymerase-δ and is a stable cell-cycle-regulated nuclear protein (synthesized mainly in the S phase but also present in G_1 and G_2 phases of the cell cycle), the presence of which correlates directly with the proliferative state of normal cells.[9,10] In our hands, PCNA immunostaining has revealed a good correlation with thymidine labeling of rat intestine[1] as well as with a different proliferation-specific antibody to Ki-67 antigen[6,11] on both human atherosclerotic plaques (coronary and carotid) and tonsil tissue.[1,8] Thus, an underlying assumption of this paper is that immunostainable PCNA denotes sites of active cell proliferation.

Recently, with the use of an anti-PCNA antibody, a low level of cell proliferation was found in human coronary arteries, both normal and atherosclerotic.[1,2] This is low compared with the maximal indices of of 30 to 50% seen with acute mechanical arterial injury,[12] but such a low level occurring over numerous years, with associated extracellular matrix production, could easily produce an occlusive arterial mass by mid-life.

In the coronary plaques, intima tended to have a slightly greater proportion of PCNA-positive cells than did media. However, these differences were not statistically significant.[1] In the current study, we found that human carotid plaques display very similar low proliferative indices. Despite these low levels of overall proliferative activity, in the carotid plaques we found that intima displayed significantly more proliferation than the underlying media. The latter is in concert with the fact that the vast majority of the other atherosclerosis-related events (lipid accumulation, hemorrhages, collagen deposition, etc) also takes place preferentially in the intima.[3]

One-time observation studies of human material are insufficient to characterize the actual time course of proliferation during the development of individual atherosclerotic plaques. At least three patterns of human atherosclerotic plaque development and growth can be proposed: (1) a single, brief proliferative burst associated with some injury at an unspecified time and followed by a long, minimal-to-absent proliferative phase (analogous to the balloon injury models[12]); (2) several similar episodes of brief proliferative bursts caused by repeated injuries; and (3) a slow growth pattern similar to that in the hypercholesterolemia models.[13–20] Our proliferative indices are similar to those reported in hypercholesterolemia models (pig and rabbit) of early atherosclerosis, and in fact, no proliferative indices above 5% have been described in these widely used model systems.[13–20] Nevertheless, this proliferative response is able to produce significantly stenotic lesions in several months to a few years. Such models may thus be representative of human atherosclerosis development, which takes several years before it can become prevalent at autopsy.[21–24]

As for human plaques of different ages, even the scant available data suggest a similar proliferative scenario. Katsuda et al[25] studied the earliest grossly identifiable lesions of the human aorta, the fatty streak, and demonstrated that less than 2% of the cells were PCNA positive. Orekhov et al[26] examined cells extracted from human aortic, relatively young (nonocclusive, uncomplicated) plaques with flow cytometry and found hardly any cells definitely in the DNA synthesis phase of the cell cycle. We found similar low levels of cell proliferation in human coronary arteries, not all of which were advanced plaques.[1] Interestingly, we did not find any differences in cell proliferation in complicated plaques derived from hearts with severe coronary artery disease and in immature plaques derived from hearts with idiopathic dilated cardiomyopathy. Therefore, we think that the low proliferative indices described in the present study rather reflect the general pattern of plaque growth and are not simply a result of the advanced age of the lesion or patient or a result of the impression that surgically removed carotid plaques are burned out. Given this, we felt it most interesting to focus on what cell types and which topographical locations display this low overall rate of cell proliferation.

Previous studies from this laboratory and others have indicated that proliferation in human atherosclerotic lesions occurs among smooth muscle cells, endothelial cells, and monocyte/macrophages.[1,2,25] In this report, we confirmed these data and also provided the first demonstration of active proliferation among CD3-positive T cells. In general, T cells in the atherosclerotic plaque may represent (1) primarily locally activated, plaque antigen-specific cells, (2) secondarily recruited, centrally activated, plaque antigen-specific cells, or (3) nonspecific, secondarily recruited cells[27] Previous analyses of human plaque T cells demonstrated a predominantly polyclonal composition arguing against major antigen-specific clonal expansions.[28,29] Our finding of local T cell proliferation, however, suggests T lymphocyte activation by local antigen presentation and opens the possibility that at least small populations of antigen-specific T cells can exist in human atherosclerotic plaques.

In the present paper, we have identified different topographical patterns of cell proliferation in human carotid plaques on the basis cell type. We demonstrated that the preponderant proliferative cell type in the intima was the monocyte/macrophage, with a minority being smooth muscle α-actin-positive, microvascular endothelial, and T cells. Smooth muscle cells were the dominant proliferating cell type in the media. Within the plaque, foam-cell-rich regions mostly displayed proliferation among macrophages, whereas in vascularized fields PCNA positivity was almost equally shared by endothelial cells, monocyte/macrophages, smooth muscle α-actin-positive cells, and to a lesser extent, T cells. Logistic and linear regression analyses also demonstrated that location in foam-cell-rich regions was a significant predictor of proliferation only among monocyte/macrophages, whereas location in vascularized regions was a good predictor of PCNA positivity among both inflammatory and noninflammatory cells.

These different patterns of cell type proliferation suggest possibly different distributions of putative responsible growth factors in human atherosclerosis. Human atherosclerotic plaques contain growth factors that can promote the proliferation of macrophages, smooth muscle cells, and endothelial cells, such as macrophage colony-stimulating factor,[30] platelet-derived growth factors AA and BB,[31,32] and acidic fibroblast growth factor.[33] Activated T cells elaborate the autocrine growth factor interleukin-2, and the presence of interleukin-2 receptors have been demonstrated in a subset of T cells in human atherosclerotic plaques.[34] We and others previously demonstrated colocalization of platelet-derived growth factor[7,31] and acidic fibroblast growth factor[33] with plaque microvessels, which corroborates cell proliferation data presented in this paper. Future studies are required for colocalization of putative

growth factors and proliferation of individual cell types in human atherosclerosis.

It is hard to evaluate the relative biological importance of the proliferation of different cell types. We think, however, that from the clinical standpoint, proliferation of noninflammatory cells (smooth muscle cells, endothelial cells, undefined mesenchymal cells, which may represent modified smooth muscle cells, as well as cells of nonmuscle lineage) has far more serious implications for overall plaque growth. As every newly formed mesenchymal cell can be a source of collagen and other extracellular matrix protein synthesis,[5,35] multiplication of such cells might contribute to the ultimate growth of the plaque volume in geometrical progression. Interestingly, our recent study revealed that vascularization is a significant independent predictor of type I collagen gene expression in human atherosclerotic plaques.[5] In the present paper, we demonstrate preferential proliferation of smooth muscle and endothelial cells in the same regions. It corroborates our recent finding that localization in vascularized regions is the best predictor for noninflammatory (CD68- and CD45-negative) cell proliferation in human carotid plaques.[7] O'Brien et al[2,36] also capitalize on microvessel-associated cell proliferation in human primary and restenotic coronary lesions. We described a very similar pattern of cell proliferation in human arteriovenous fistulas used for hemodialysis.[4] Taken together, these observations indicate that neovascularization might be an important mechanism of atherosclerotic plaque progression. Therefore, elucidation of molecular and cellular mechanisms of neoangiogenesis and neoangiogenesis-driven growth of atherosclerotic plaques may lead to effective methods for treatment of advanced human atherosclerosis and, probably, other forms of vascular stenosis.

Acknowledgments

We thank the Vascular Surgery Divisions of the University of Washington and the University of Michigan for providing us with the carotid artery specimens used in this study. We also thank Bascom Brown for his technical assistance in tissue processing and sectioning.

References

1. Gordon D, Reidy MA, Benditt EP, Schwartz SM: Cell proliferation in human coronary arteries. Proc Natl Acad Sci USA 1990, 87:4600–4604
2. O'Brien ER, Alpers CE, Stewart DK, Ferguson M, Tran N, Gordon D, Benditt EP, Hinohara T, Simpson JB, Schwartz SM: Proliferation in primary and restenotic coronary atherectomy tissue: implications for antiproliferative therapy. Circ Res 1993, 73:223–231
3. Van Damme H, Vivario M, Boniver J, Limet R: Histologic characterization of carotid plaques. Cardiovasc Pathol 1994, 3:9–17
4. Rekhter M, Nicholls S, Ferguson M, Gordon D: Cell proliferation in human arteriovenous fistulas used for hemodialysis. Arterioscler Thromb 1993, 13: 609–617
5. Rekhter MD, Zhang K, Narayanan AS, Phan S, Schork MA, Gordon D: Type I collagen gene expression in human atherosclerosis: localization to specific plaque regions. Am J Pathol 1993, 143:1634–1648
6. Cattoretti G, Becker MH, Key G, Duchrow M, Schluter C, Galle J, Gerdes J: Monoclonal antibodies against recombinant parts of the Ki-67 antigen (MIB 1 and MIB 3) detect proliferating cells in microwave-processed formalin-fixed paraffin sections. J Pathol 1992, 168: 357–363
7. Rekhter MD, Gordon D: Does platelet-derived growth factor-A chain stimulate proliferation of arterial mesenchymal cells in human atherosclerotic plaques? Circ Res 1994, 75:410–417
8. Rekhter MD, Gordon D: Cell proliferation and collagen synthesis are two independent events in human atherosclerotic plaques. J Vasc Res 1994, 31:280–286
9. Kurki P, Vanderlaan M, Dolbeare F, Gray J, Tan EM: Expression of proliferating cell nuclear antigen (PCNA)/cyclin during the cell cycle. Exp Cell Res 1986, 166: 209–219
10. Bravo R, Frank R, Blundell PA, Macdonald-Bravo H: Cyclin/PCNA is the auxiliary protein of DNA polymerase-δ. Nature 1987, 326:515–517
11. Gerdes J, Schwab U, Lemke H, Stein H: Production of a mouse monoclonal antibody reactive with a human nuclear antigen associated with cell proliferation. Int J Cancer 1983, 31:13–20
12. Clowes AW, Reidy MA, Clowes MM: Kinetics of cellular proliferation after arterial injury. I. Smooth muscle growth in the absence of endothelium. Lab Invest 1983, 49:327–333
13. Rosenfeld ME, Ross R: Macrophage and smooth muscle cell proliferation in atherosclerotic lesions of WHHL and comparably hypercholesterolemic fat-fed rabbits. Arteriosclerosis 1990, 10:680–687
14. Kim DN, Schmee J, Lee KT, Thomas WA: Atherosclerotic lesions in the coronary arteries of hyperlipidemic swine. I. Cell increases, divisions, losses and cells of origin in first 90 days on diet. Atherosclerosis 1987, 64:231–242
15. Kim DN, Imai H, Schmee J, Lee KT, Thomas WA: Intimal cell mass-derived atherosclerotic lesions in the abdominal aorta of hyperlipidemic swine. I. Cell of origin, cell divisions and cell losses in first 90 days on diet. Atherosclerosis 1985, 56:169–188

16. Scott RF, Thomas WA, Kim DN, Schmee J: Endothelial cell labeling indices in swine aortas in relation to intimal cell mass-derived atherosclerotic lesions. Atherosclerosis 1985, 56:263–270
17. Kim DN, Schmee J, Ho HT, Thomas WA: The "turning off" of excessive cell replicative activity in advanced atherosclerotic lesions of swine by a regression diet. Atherosclerosis 1988, 71:131–142
18. Florentin RA, Nam SC, Daoud AS, Jones R, Scott RF, Morrison ES, Kim DN, Lee KT, Thomas WA, Dodds WJ, Miller KD: Dietary-induced atherosclerosis in miniature swine. Exp Mol Pathol 1968, 8:263–301
19. Walker LN, Reidy MA, Bowyer DE: Morphology and cell kinetics of fatty streak lesion formation in the hypercholesterolemic rabbit. Am J Pathol 1986, 125:450–459
20. Florentin RA, Nam SC, Lee KT, Lee KJ, Thomas WA: Increased mitotic activity in aortas of swine after three days of cholesterol feeding. Arch Pathol 1969, 88: 463–469
21. Stary HC: Evolution and progression of atherosclerotic lesions in coronary arteries of children and young adults. Arteriosclerosis 1989, 9:I19-I32
22. Velican C, Velican D: Progression of coronary atherosclerosis from adolescents to mature adults. Atherosclerosis 1983, 47:131–144
23. Geer JC, McGill HC Jr, Robertson WB, Strong JP: Histologic characteristics of coronary artery fatty streaks. Lab Invest 1968, 18:565–570
24. Solberg LA, Strong JP: Risk factors and atherosclerotic lesions: a review of autopsy studies. Arteriosclerosis 1983, 3:187–198
25. Katsuda S, Coltrera MD, Ross R, Gown AM: Human atherosclerosis. IV. Immunocytochemical analysis of cell activation and proliferation in lesions of young adults. Am J Pathol 1993, 142:1787–1793
26. Orekhov AN, Kosykh VA, Repin VS, Smirnov VN: Cell proliferation in normal and atherosclerotic human aorta. I. Flow cytofluorometric determination of cellular deoxyribonucleic acid content. Lab Invest 1983, 48:395–398
27. Stemme S, Hansson GK: Immune mechanisms in atherosclerosis. Coronary Artery Dis 1994, 5:216–222
28. Stemme S, Rymo L, Hansson GK: Polyclonal origin of T lymphocytes in human atherosclerotic plaques. Lab Invest 1991, 65:654–660
29. Swanson SJ, Rosenzweig A, Seidman JG, Libby P: Diversity of T-cell antigen receptor V β gene utilization in advanced human atheroma. Arterioscler Thromb 1994, 14:1210–1214
30. Clinton SK, Underwood R, Hayes L, Sherman ML, Kufe DW, Libby P: Macrophage colony-stimulating factor gene expression in vascular cells and in experimental and human atherosclerosis. Am J Pathol 1992, 140: 301–316
31. Wilcox JN, Smith KM, Williams LT, Schwartz SM, Gordon D: Platelet-derived growth factor mRNA detection in human atherosclerotic plaques by *in situ* hybridization. J Clin Invest 1988, 82: 1134–1143
32. Ross R, Masuda J, Raines EW, Gown AM, Katsuda S, Sasahara M, Malden LT, Masuko H, Sato H: Localization of PDGF-B protein in macrophages in all phases of atherogenesis. Science 1990, 248: 1009–1012
33. Brogi E, Winkles JA, Underwood R, Clinton SK, Alberts GF, Libby P: Distinct patterns of expression of fibroblast growth factors and their receptors in human atheroma and nonatherosclerotic arteries. J Clin Invest 1993, 92:2408–2418
34. Stemme S, Holm J, Hansson GK: T lymphocytes in human atherosclerotic plaques are memory cells expressing CD45RO and the integrin VLA-1. Arterioscler Thromb 1992, 12:206–211
35. Liptay MJ, Parks WC, Mecham RP, Roby J, Kaiser LR, Cooper JD, Botney MD: Neointimal macrophages colocalize with extracellular matrix gene expression in human atherosclerotic pulmonary arteries. J Clin Invest 1993, 91:588–594
36. O'Brien ER, Garvin MR, Dev R, Stewart DK, Hinohara T, Simpson JB, Schwartz SM: Angiogenesis in human coronary atherosclerotic plaques. Am J Pathol 1994, 145:883–894